ELSEVIER

Contents lists available at ScienceDirect

Science of the Total Environment

journal homepage: www.elsevier.com/locate/scitotenv





Global biomass maps can increase the precision of (sub)national aboveground biomass estimates: A comparison across tropical countries

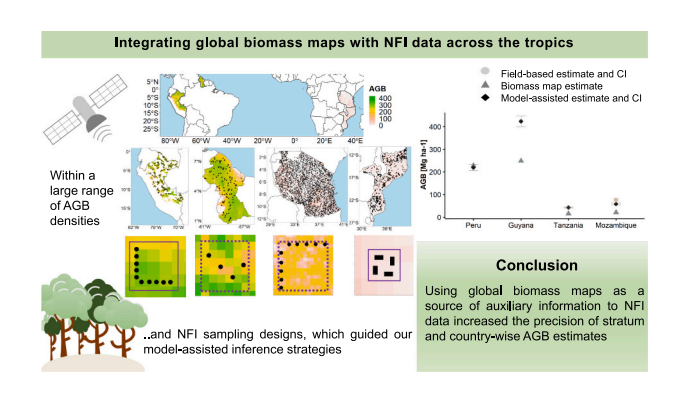
Natalia Málaga ^{a,*}, Sytze de Bruin ^a, Ronald E. McRoberts ^{b,c}, Erik Næsset ^d, Ricardo de la Cruz Paiva ^e, Alexs Arana Olivos ^e, Patricia Durán Montesinos ^e, Mahendra Baboolall ^f, Hercilo Sancho Carlos Odorico ^g, Muri Gonçalves Soares ^g, Sérgio Simão Joã ^g, Eliakimu Zahabu ^h, Dos Santos Silayo ⁱ, Martin Herold ^{a,j}

- a Laboratory of Geo-Information Science and Remote Sensing, Wageningen University and Research, Droevendaalsesteeg 3, 6708, PB, Wageningen, the Netherlands
- ^b Raspberry Ridge Analytics, Hugo, MN 55038, USA
- ^c Department of Forest Resources, University of Minnesota, Saint Paul, MN 55108, USA
- ^d Faculty of Environmental Sciences and Natural Resource Management, Norwegian University of Life Sciences, NO-1432 Ås, Norway
- ^e Servicio Nacional Forestal y de Fauna Silvestre, Ministerio de Desarrollo Agrario y Riego (SERFOR), Lima, Peru
- f Forest Carbon Monitoring, REDD Department, Guyana Forestry Commission, Georgetown, Guyana
- 8 Measurement, Reporting, and Verification Unit, National Sustainable Development Fund (FNDS), Av. Vladimir Lenine, No. 174, 16th Floor, Block A (Millennium Park), Maputo City, Mozambique
- h College of Forestry Wildlife and Tourism, Sokoine University of Agriculture, P.O. Box 3013, Morogoro, Tanzania
- ⁱ Tanzania Forest Services (TFS) Agency, Ministry of Natural Resources and Tourism Box 2228, Itega Dodoma, Tanzania
- ^j Helmholtz Center Potsdam GFZ German Research Centre for Geosciences, Section 1.4 Remote Sensing and Geoinformatics, Telegrafenberg, Potsdam 14473, Germany

HIGHLIGHTS

- Global maps increase the precision of field-based AGB estimates across the tropics.
- Uncalibrated global biomass maps unfit for country carbon reporting.
- Two-stage model-assisted estimators qualify for common NFI clustered plot designs.
- Estimation specifics depend on interplot distance relative to map unit size.
- While country-specific solutions are necessary, cross-country lessons were learned.

G R A P H I C A L A B S T R A C T



ARTICLE INFO

Editor: Kuishuang Feng

Keywords: Global biomass map National forest inventory

ABSTRACT

Countries within the tropics face ongoing challenges in completing or updating their national forest inventories (NFIs), critical for estimating aboveground biomass (AGB) and for forest-related greenhouse gas (GHG) accounting. While previous studies have explored the integration of map information with local reference data to fill in data gaps, limited attention has been given to the specific challenges presented by the clustered plot designs frequently employed by NFIs when combined with remote sensing-based biomass map units. This research

E-mail address: natalia.malagaduran@wur.nl (N. Málaga).

https://doi.org/10.1016/j.scitotenv.2024.174653

^{*} Corresponding author.

Sampling design Plot configuration Model-assisted inference addresses these complexities by conducting four country case-studies, encompassing a variety of NFI characteristics within a range of AGB densities. Examining four country case-studies (Peru, Guyana, Tanzania, Mozambique), we assess the potential of European Space Agency's Climate Change Initiative (CCI) global biomass maps to increase precision in (sub)national AGB estimates. We compare a baseline approach using NFI field-based data with a model-assisted scenario incorporating a locally calibrated CCI biomass map as auxiliary information.

The original CCI biomass maps systematically underestimate AGB in three of the four countries at both the country and stratum level, with particularly weak agreement at finer map resolution. However, after calibration with country-specific NFI data, stratum and country-level AGB estimates from the model-assisted scenario align well with those obtained solely from field-based data and official country reports. Introducing maps as a source of auxiliary information fairly increased the precision of stratum and country-wise AGB estimates, offering greater confidence in estimating AGB for GHG reporting purposes.

Considering the challenges tropical countries face with implementing their NFIs, it is sensible to explore the potential benefits of biomass maps for climate change reporting mechanisms across biomes. While country-specific NFI design assumptions guided our model-assisted inference strategies, this study also uncovers transferable insights from the application of global biomass maps with NFI data, providing valuable lessons for climate research and policy communities.

1. Introduction

NFIs have been developed to flexibly assess forest resources, accommodating the unique environmental characteristics specific to a region (i.e. topography, climate, forest types); their needs (i.e. commercial interests, financial restrings) and rates of change (McRoberts et al., 2012). Consequently, NFIs around the world exhibit variations in their definitions of a forest, sampling designs (such as systematic vs. random sampling, stratification strategies, among others), and plot configurations (Nesha et al., 2022). Moreover, NFIs have evolved beyond their original purpose of solely assessing commercial timber inventory; they now include variables such as carbon pools and biodiversity, which have introduced further complexity to plot configurations (Lawrence et al., 2010). As a result, NFIs use plots of varying sizes, shapes, and numbers. To enhance logistical efficiency, NFIs often adopt clusters composed of plots in close proximity (Lawrence et al., 2010).

More recently, continuous advancements in remote sensing technologies have led several countries to adopt remote sensing-based products for monitoring and reporting forest cover and changes (Romijn et al., 2015). Yet, only a few have explored the application of biomass maps under UNFCCC reporting schemes, often with indirect applications (Melo et al., 2023). Open access, coarse-scale biomass maps have actually been available for over a decade (Avitabile et al., 2016; Saatchi et al., 2011; Baccini et al., 2012), and ongoing dedicated spacebased biomass missions, such as the European Space Agency's BIOMASS and NASA's GEDI, are expected to further improve biomass mapping (Ochiai et al., 2023). Recognizing the potential of this influx of data, the 2019 Refinement to the 2006 Intergovernmental Panel on Climate Change (IPCC) Guidelines for National Greenhouse Gas Inventories (Ogle et al., 2019) endorsed the incorporation of biomass maps into GHG inventories and reporting schemes. While some studies have used biomass maps to enhance national aboveground biomass (AGB) estimates (Bullock et al., 2023; Málaga et al., 2022), more examples are needed to build confidence and understand the extent to which remote sensing-based products can effectively support GHG monitoring and reporting. However, integrating remote sensing information with data from cluster plot configurations remains challenging. In this research, we probe the complexities around the integration of global biomass map with NFI data under model-assisted inference across four tropical country case-studies: Peru, Guyana, Mozambique, and Tanzania. These selected countries not only represent a spectrum of NFI characteristics but also encompass diverse biomass density ranges. One common element among these countries, though, is the use of clusters of plots with some form of fixed arrangement of plots within those clusters.

Given the difficulties tropical countries encounter in completing or updating their NFIs (Nesha et al., 2022), it is crucial to explore the benefits model-assisted estimation can offer as well as understanding the

challenges faced under diverse NFI sampling designs prevalent in the tropics. The model-assisted framework relies on a probabilistic sample of reference data, such as acquired by NFIs, in combination with auxiliary information, nowadays typically based on remotely sensed data. Model-assisted estimation has been shown to increase the precision of forest-related estimates (i.e. growing stock volume, AGB) (Ståhl et al., 2016; Næsset et al., 2016, 2020). While the use of maps in the context of the model-assisted estimation has been explored extensively, little attention has been devoted to ways of accommodating NFI cluster plot configurations and the corresponding map units when establishing a map-to-plot regression model. A pertinent concept to explore when working with clustered plots under model-assisted estimation is the twostage sampling framework described by Särndal et al. (1992) and elaborated by McRoberts et al. (2024). Under two-stage sampling, the population or area of interest is assumed to be tessellated into first-stage units which, in turn, are tessellated into second-stage units or population elements. In the first stage of sampling, primary sampling units (PSUs) are assumed to be selected at random from the first-stage population units. In the same line, the selection of secondary sampling units (SSUs) is assumed to be done at random from within the selected PSUs; although in most NFIs, plots (i.e. SSUs) are arranged in some kind of fixed spatial configuration. Särndal et al. (1992) present two main cases that apply to the map-to-plot relationship assessed in the current study: i) case A, where the regression model is built between PSU-level mean estimates (e.g. between mean AGB values over plots of the same cluster as the dependent variable and PSU-level map values as the independent variable); and ii) case B, where the model relationship is defined at the SSU level (e.g. between the individual AGB plot values as the dependent variable and individual AGB map unit values as the independent variable). Málaga et al. (2022) and Næsset et al. (2020, 2016) also addressed applications of case A and case B model-assisted estimators but without explicitly referring to them as such.

The objectives of this study were to demonstrate the practicalities of model-assisted approaches and to assess the extent to which they may increase the precision of (sub)national AGB estimates using global biomass maps as auxiliary information. Specifically, using four country case-studies, the current research addresses: i) selecting the form of the model-assisted estimator that accommodates a country's specific NFI sampling design and plot configuration; ii) assessing the extent to which a locally calibrated global biomass product increases the precision of (sub)national AGB estimates in different biomes (low vs. high biomass); and iii) identifying the main map-to-plot harmonization challenges that countries face when integrating biomass map information with NFI data. To evaluate the effects of the global map on the precision of (sub)national AGB estimates, we compared baseline scenarios solely relying on the country's NFI field-based information to model-assisted scenarios applying the global biomass map, locally calibrated using NFI data. The

AGB estimates obtained in this study serve the specifically stated research objectives and may not align with the official country reports.

2. Material and methods

2.1. Global biomass maps

The European Space Agency Climate Change Initiative (CCI) version 4 (v4) global biomass maps (Santoro and Cartus, 2023), expressed in AGB, were used as a source of auxiliary information to the countries' NFI data. In the case of Tanzania, we used the 2010 map, whereas, for Peru, Guyana and Mozambique the 2017 map was selected. We chose the map epochs closest to the countries' NFI implementation timeframes to minimize potential discrepancies caused by temporal mismatches (Duncanson et al., 2021). The 2017 epoch map was constructed by merging data from Synthetic Aperture Radar (SAR) C-band Sentinel-1, and Phased Array L-band SAR (PALSAR-2) obtained from ALOS-2, along with other remote sensing sources; whereas the 2010 epoch is based on datasets of ALOS-1 PALSAR-1 and Envisat ASAR (Santoro and Cartus, 2023). Country-wise corresponding map tiles with ~100 m resolution were downloaded from the ESA biomass CCI repository (Santoro and Cartus, 2023). In this study, the biomass maps were used solely as an auxiliary information source, so the accompanying uncertainty layers to the maps were not used.

2.2. Country NFI sampling designs and ground-based information

2.2.1. Peru

The National Forest and Wildlife Inventory (NF&WI) of Peru divided the country into six strata. Only four strata confined to the Peruvian Amazonia are part of this study: hydromorphic zone (HZ), accessible montane forest (AMF), inaccessible montane forest (IMF), and lowland forest (LF). The NF&WI follows a non-aligned systematic sampling design, in which an L-shaped cluster is randomly selected within a grid cell whose size varies depending on the stratum (MINAGRI and MINAM, 2016). Because of the financial and logistic complexity of the NF&WI's implementation, the inventory is executed in five panels. A panel consists of a selection of grouped contiguous grid cells distributed over a stratum; the groups belonging to a panel are assumed to be a random sample of a stratum. As the process continues, each subsequent panel follows the same approach, comprising roughly 20 % of the sample from its respective stratum. The NF&WI only visits clusters that are at least partially forested according to a remotely sensed land cover assessment using fine-resolution imagery (MINAGRI and MINAM, 2016). Between 2013 and 2020, approximately 32 % of the NF&WI's total sample had been measured in Peru, with most of the work restricted to panels 1 and 2. Some plots within these panels were considered missing at random. As in Málaga et al. (2022), the area of interest in this study is restricted to only those grid cells in panels 1 and 2 within the Peruvian Amazonia forestland (Fig. 1b), from which the clusters are deemed a random sample.

In the NF&WI, a cluster consists of seven to 10 plots configured in the

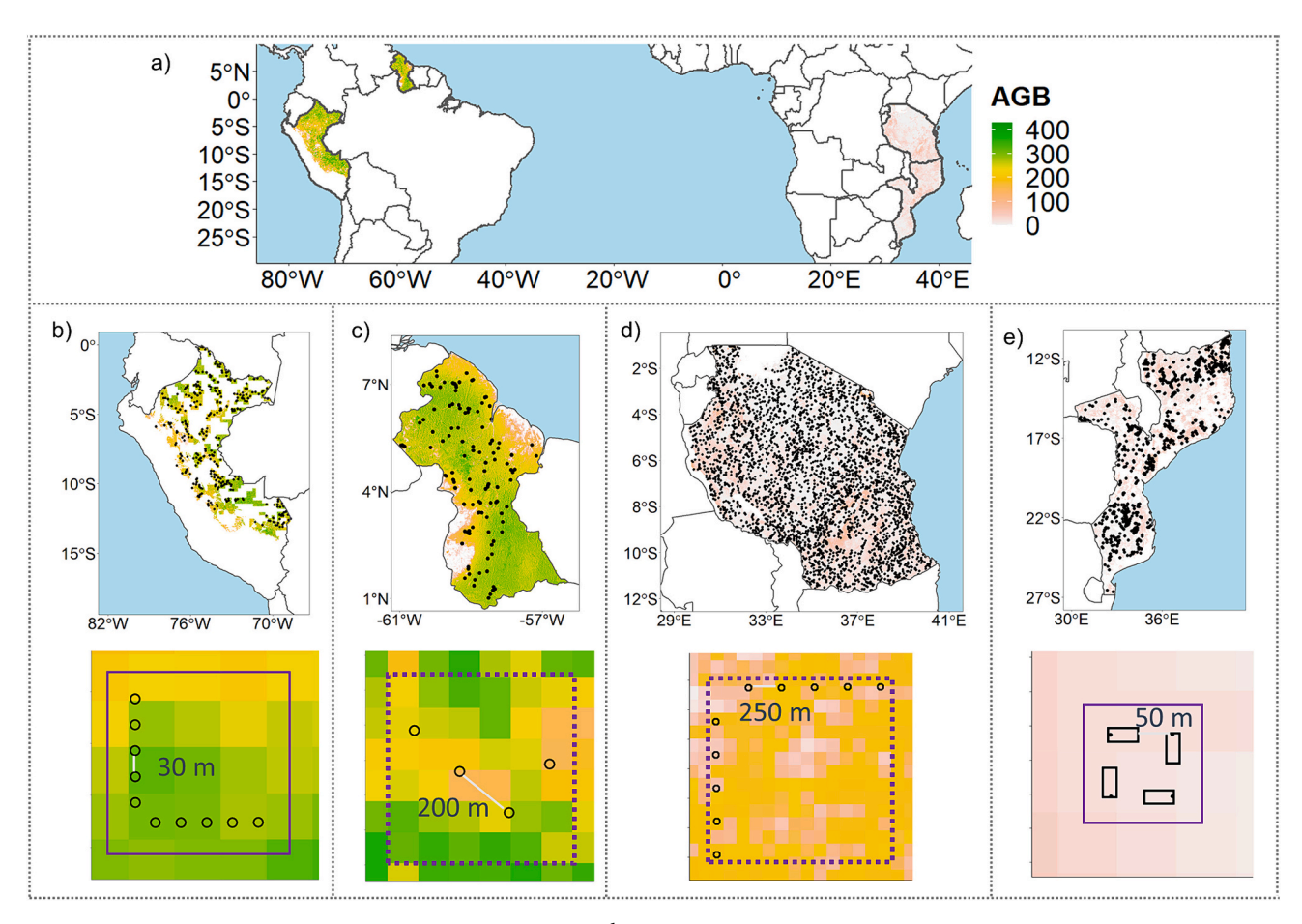


Fig. 1. Selected countries and their respective CCI biomass maps (in Mg ha⁻¹) and NFI reference data. In the top panel (a), country cut-outs of the CCI biomass map are displayed in the background. The center row shows the reference data and the CCI biomass maps to the extent of the population as defined for Peru (b), Guyana (c), Tanzania (d) and Mozambique (e), respectively. The bottom row details examples of these countries' plot configurations along with our defined polygons circumscribing a cluster (PSUs) (in continuous purple lines for our model-assisted case A countries and dotted purple lines for our model-assisted case B countries, elaborated in Section 2.4).

shape of an L, with one side consistently facing north and the other east. Within the HZ, AMF and IMF strata, 10 circular plots of 0.05 ha in size constitute a cluster, while in the lowland forest stratum the clusters are composed of seven rectangular plots of 50 m \times 20 m (0.1 ha) each (Appendix A, Fig. A.1a and b, respectively) (MINAGRI and MINAM, 2016). The NF&WI provided tree-level (of DBH \geq 10 cm) live-woody AGB for the 299 clusters (32 in HZ; 46 in AMF; 11 in IMF and 210 in LF) used in this study. Cluster-level AGB was predicted using the BIOMASS R package (Réjou-Méchain et al., 2017). More details on the cluster-level AGB predictions and data pre-processing analysis are described in Málaga et al. (2022).

2.2.2. Mozambique

A restricted stratified random sampling approach was followed, with the strata based on the four main forest types of the country, according to a 2008 re-classified agro-ecological map (MITADER, 2018). The distinguished forest strata are: Mopane (Mo), Mecrusse (Me), Semideciduous forest (SDF) and Semi-evergreen forests (SEF). The optimal allocation approach was followed, and within each stratum the sampling intensity was proportional to the area and variability within the stratum (MITADER, 2018). Plot locations were initially randomly selected within each stratum, but later the decision was made to move the random locations to grid intersections (Government of Mozambique, 2018). In most regions, the minimum distance between sampling units was 4 km, with the exception of the provinces of Cabo Delgado and Gaza, where it was 1 km. Upon visual inspection of the sampling units, some clusters of the original design were re-located, because the stratification map turned out to be too coarse and had discrepancies between the map vegetation classes and the ground conditions (Alegria, 2020).

Each cluster consists of four 50 m \times 20 m (0.1 ha) plots at 50 m spacing configured in a square (Figs. 1e and A.1c, Appendix A), each subdivided in four subplots of 25 m \times 10 m. All trees with DBH >10 cm were measured within a plot and trees with DBH >5 cm and lower than 10 cm were measured within the first subplot (MITADER, 2018). For the analysis, a dataset with AGB information for 3420 plots, was obtained from the publicly accessible Plataforma de acompanhamento dos Projectos website (Fundo Nacional de Desenvolvimento Sustentavel, n.d.). Pre-processing of the reference data involved filtering out clusters with missing or duplicated coordinates. Additionally, clusters that did not fall within the four forest strata as defined by the re-classified Agroecological map (our area of interest) were disregarded, assuming they had been moved and departed from the original design. Clusters crossing stratum boundaries were assigned to the majority stratum. Our analysis involved 721 complete clusters.

2.2.3. Tanzania

In Tanzania, the NFI followed a double-sampling for stratification design (Tomppo et al., 2014). In the first phase, a North to South, 5 km \times 5 km grid was laid over mainland Tanzania. The Northwest corner of each grid cell was the cluster anchor point (Næsset et al., 2020) (Fig. 1d). Based on the predicted growing stock volume, slope and time-measurement criteria, every anchor point was assigned to one of 18 mutually exclusive strata (Tomppo et al., 2014). In the second phase, the sample units were systematically selected from the initial grid. The sampling intensity differed among strata. In the most intensively sampled stratum, a cluster was selected every 5 km, while in the least intensively sampled a cluster was selected every 45 km (MNRT, 2015).

Following the implementation of the NFI, the Food and Agricultural Organization of the United Nations (FAO) created a spatially continuous stratification layer, following the same stratification criteria as the country's original design (Anssi Pekkarinen, pers.comm.). In a recent study, Næsset et al. (2020) reported consistency between the reconstructed stratification map and the stratum classes of the second-phase sample for a specific area of the country. We assumed such consistency also holds for the extent of our study. Following Næsset et al. (2020), we adopted the stratification layer to define the strata of the

reference data and overall population units, meaning that we also consider a single-phase stratified systematic design for Tanzania. Having a spatially continuous stratification layer allows us to use the global biomass map as a source of auxiliary information in our model-assisted approach. Moreover, Tanzania's NFI recorded information for trees both in and outside forestlands, hence our area of interest constitutes the mainland territory of the country (URT, 2010).

In Tanzania, six to 10 circular plots (0.07 ha) following an inverse Lshaped configuration constitute a cluster, depending on the type of forest in a stratum. The distance between adjacent plots within the same cluster is 250 m (Fig. A.1d, Appendix A). The individual plots are nested, formed by 1-, 5-, 10- and 15-m radius concentric circular subplots, where smaller trees (DHB > 1 cm) were measured in the smallest subplots and larger trees (DBH > 20 cm) within the entire plot (MNRT, 2015). Our analysis was conducted on the 2010–2013, plot-level, livetree AGB (Mg \mbox{ha}^{-1}), ground-based information collected as part of the National Forest Resources Monitoring and Assessment (NAFORMA) program led by Tanzania Forest Services (TSF) Agency, in collaboration with the FAO-Finland forestry program (MNRT, 2015). All plots within the same cluster were assigned to a single stratum corresponding to that of the northwest corner of a cluster's bounding box. Additional reference data preparation procedures involved the exclusion of plots with erroneously duplicated coordinates. The analysis was conducted on 3208 clusters with a total of 30,382 plots distributed over 18 strata.

2.2.4. Guyana

Guyana's National Forest Carbon Monitoring System (FCMS) originally defined a stratified two-stage list sampling design. Sampling was carried out in six strata defined by potential for change and accessibility criteria: high potential for change and more accessible forest (HPC/MA), high potential for change but less accessible forest (HPC/LA), medium potential for change and more accessible forest (MPC/MA), medium potential for change but less accessible forest (MPC/LA), low potential for change and more accessible forest (LPC/MA), and low potential for change but less accessible forest (LPC/LA) (Brown et al., 2014). Following the FCMS, forests within these six strata represent our area of interest. In the first stage, stratified sampling was conducted by randomly selecting cells from a 10 km \times 10 km grid laid across the country, with probability of selection proportional to the area of the stratum of interest within the grid cells (Brown et al., 2014). In the second stage, the anchor point of a cluster was randomly allocated inside the selected grid cell. The 10 km \times 10 km cells are very large compared to the dimensions of the cluster (400 m \times 200 m), whose plots hence cannot be considered a random sample of the entire cell. To facilitate statistical estimation across scenarios, we adopted an alternative view on the sampling design. We assumed a rectangular polygon large enough to encompass the cluster (6×6 CCI biomass map units) as the first stage sampling unit. We used the original proportions of the stratum of interest within the 10 km \times 10 km grid cell to account for the unequal selection probabilities into our first stage analyses of AGB mean and variances (Section 2.5). The plots composing the cluster were assumed to represent a random sample of the population units inside the first stage sampling unit.

Every cluster consists of four circular plots (0.126 ha) fixed in an L-shaped form with random orientation, separated by 200 m or 400 m from the cluster's anchor point (Figs. 1c and A.1e, Appendix A). Plots were nested. Trees with DBH between 5 and 25 cm were recorded within a smallest radius subplot (6 m) and those with DBH > 25 cm within the entire plot. We used data from 472 plots provided by Guyana's Forestry Commission and measured between 2011 and 2019. All plots within the same cluster were assigned to a single stratum by overlaying the stratification map provided by the country to the cluster's anchor point. One cluster was deleted due to having duplicate coordinates. Additionally, aboveground carbon (in the form the information was originally provided) was converted to AGB using a conversion factor of 0.49 t C (tonne d.m.) $^{-1}$ (Aalde et al., 2006, Vol. 4, Chap 4, Section 4.5).

2.3. Defining the map-to-plot assessment strategy and the regression model

To assess the contribution of the biomass map to (sub)national AGB estimates, we employed model-assisted regression estimators and compared the results with a baseline approach. In the latter, the estimates relied solely on field-based data from the country's NFI. In contrast, the model-assisted estimates integrated a locally calibrated biomass map as auxiliary information. For each country, we developed linear regression models to predict AGB (Mg ha⁻¹) for every map unit, using the CCI biomass map unit values as the independent variable.

A common element regarding plot configuration across countries is the use of clusters with plots arranged in some kind of fixed configuration. The size, shape and orientation of those clusters and plots and the distance between them vary considerably, occasionally also within a country (Table 1). In the case of Peru and Mozambique, the distance between plots of the same cluster is less than the size of the CCI map units (~100 m), whereas for Tanzania and Guyana it is at least 200 m. If two or more plots occur within the same biomass map unit, the 1:1 relationship between the map units and plots needed for establishing a regression model under the two-stage model-assisted estimation framework is disrupted (Särndal et al., 1992, Chapter 8). In that case, (i. e. for Peru and Mozambique) model-assisted case A as formulated by Särndal et al. (1992, p. 304) was followed; whereas for Tanzania and Guyana, we implemented case B (Table 1) Särndal et al. (1992, p. 305).

An important distinction between case A and B relates to the level of aggregation at which the regression model associating map and field-based AGB is fitted within each stratum, h. Referring to the terminology of the introduction, a PSU here consists of a square polygon whose dimensions are large enough to encompass all plots within a cluster, where the plots are the SSUs. In case A, the dependent variable, \bar{y}_i , corresponds to the mean AGB over the plots within the i^{th} PSU and the independent variable, \hat{y}_i , is the mean AGB over the CCI biomass map units within the i^{th} PSU (Eq. (1)). In case B, as opposed to case A, the dependent variable, y_{ij} , is the individual AGB estimate at the j^{th} plot within the i^{th} PSU and the independent variable, \hat{y}_{ij} , is the matching in location AGB individual map unit value (Eq. (2)). In case A, the auxiliary information (i.e. the CCI biomass map) is used to predict AGB country-fitted map values over map units aggregated to PSU-sized whereas in case B the individual map units are used.

$$\overline{\mathbf{y}}_{hi} = \beta_{0h} + \beta_{1h} \hat{\mathbf{y}}_{hi} + \varepsilon_{hi} \tag{1}$$

$$y_{hij} = \beta_{0h} + \beta_{1h} \hat{y}_{hij} + \varepsilon_{hij}$$
 (2)

Note that for some strata within Mozambique and Tanzania, the residuals of the selected linear models exhibited non-negligible heteroscedasticity according to the Breusch-Pagan test (Zeileis and Hothorn, 2002), for which we corrected following the procedure described in McRoberts et al. (2016). i) After fitting the model in Eq. (1) or Eq. (2), we computed the residuals (r_i) as the difference between the field-based observations $(\widehat{AGB_i})$ and the model predictions $(\widehat{AGB_i})$; (ii) the pairs

 (\widehat{AGB}_i, r_i) were sorted with respect to the model predictions \widehat{AGB}_i ; iii) the pairs were aggregated into groups of size 18 or 25 (in Mozambique and Tanzania, respectively); iv) within each group, we calculated the standard deviation of the residuals (r_i) and the mean of the model predictions (\widehat{AGB}_i) ; v) a relationship between the group standard deviations and the group predictions was used to predict the variance, the inverse of the predicted variance was used to weight each observation when refitting the model in Eq. (1) or Eq. (2).

2.4. Data harmonization procedures

Necessary harmonization procedures were followed to circumscribe the CCI biomass maps to the per-country area of interest, as previously defined in Section 2.2. For instance, in Peru, the population is restricted to forested sites within the sections of the Peruvian Amazon where the NFI has made progress. Two additional sources of auxiliary information were needed to align the wall-to-wall CCI biomass map to the aforementioned definition; a 2016 land use mask (Plataforma Geobosques, 2021) and the NFI original grid (SERFOR, 2016) representing the NFI progress in panels.

As previously mentioned, PSUs are polygons large enough to encompass all plots within a cluster. In Peru and Mozambique, PSUs selected into the sample were re-constructed to circumscribe the cluster. In Peru, the southwest corner of the polygons was positioned 50 m south and 50 m west of each cluster's anchor point (Málaga et al., 2022) (Fig. 1b). In Mozambique, the polygon was located 40 m south and 40 m west of the anchor point of every lower-left plot (Fig. 1e). We intersected the constructed polygons with the CCI biomass map units and computed the AGB density as the area-weighted mean, ignoring any potential nonforest (NA) pixels. To obtain PSU-equivalent map AGB estimates for the population, CCI map units were aggregated into polygons of the same size as the aforementioned PSUs. In Peru, this implied aggregation to 4 \times 4 or 5 \times 5 map units (size depending on the stratum) whereas in Mozambique, the aggregation concerned 2 \times 2 map units.

Similarly, a PSU in Tanzania consists of a square polygon whose dimensions approximate the length of the cluster (14×14 CCI biomass map units). As previously addressed, in Guyana we imposed the PSU to be a square polygon with a side length similar to the length of the cluster (6×6 CCI biomass map units). Most importantly, for both countries, the map-to-plot intercomparison is done among individual plots and map units (case B, Särndal et al., 1992, p. 305). For practical purposes, we associated an NFI plot with the CCI biomass map unit that contained the plot center, even though the footprint of the plot may be smaller or extend beyond the boundaries of a single map unit.

Additional map pre-processing and harmonization procedures included:

Re-projection. The field-based information, the biomass map and any
additional auxiliary information provided by the countries were reprojected to the projection system of choice of the country. In Peru
we worked on WGS 1984/UTM zone 18S; in Tanzania on WGS 1984/

Table 1Key features of the four NFIs and country-specific assumptions made under the framework of this study (the two bottom rows).

Criterion	Peru	Mozambique	Tanzania	Guyana	
Biomass density	High	Low	Low	High	
Implementation period	2013-ongoing	2015–2017	2010-2013	2011-2019	
Number of strata	4 out of 6	4	18	6	
Minimum distance between plots (m)	30 and 75	50	250	200	
Plot size (ha)	0.05 and 0.1	0.1	0.07	0.126	
Original sampling design	Stratified non-aligned systematic sampling design	Stratified random design, constrained by distance	Systematic double-phase stratified design	Two-stage stratified design	
Adaptations for implementation, per stratum	Random sample as in panel 1 and 2 within forested sites	Random sample	Single-phased random sample	Random sample	
Model-assisted estimator	Two-stage case A	Two-stage case A	Two-stage case B	Two-stage case B	

UTM zone 36S; whereas in Guyana and Mozambique on WGS 1984 Geographic Coordinate System.

- Resampling. All other auxiliary information such as the country's stratification rasters (e.g. Tanzania) or forest mask (e.g. the 2016 land-use mask of Peru, Plataforma Geobosques, 2021) was resampled to the same unit as the biomass map (~100 m × 100 m) by majority (mode).
- Cropping and masking the biomass map to the extent of each country's area of interest.

2.5. Estimators

Across all scenarios (whether field-based or model-assisted), we assumed two-stage sampling designs with some country-specific considerations. The within-PSU (second-stage) variability was deemed negligible compared to the overall variability within strata, which is consistent with Lohr (2010, Section 5.3). In an exploratory analysis of data from Tanzania and Guyana (Appendix B), this assumption was corroborated; within-PSU variability accounted for $<\!0.5$ % and 0.06% of the total variability, respectively.

2.5.1. Peru and Mozambique

For both Peru and Mozambique, we built upon a previous study in the Peruvian Amazon (Málaga et al., 2022). For the field-based scenario, we implemented a simple expansion estimator (Eqs. (3) and (4)), assuming the clusters are a random sample from each stratum (McRoberts et al., 2020).

For a single stratum, a simple expansion estimator for the mean is expressed as:

$$\widehat{\mu}_h = \frac{1}{n_h} \sum_{i=1}^{n_h} \overline{y}_{hi} \tag{3}$$

where $\bar{y}_{hi} = \frac{1}{m_{hi}} \sum_{j=1}^{m_{hi}} y_{hij}$, y_{hij} is the AGB observation for the j^{th} plot in the i^{th} PSU, m_{hi} is the number of plots within the i^{th} PSU in stratum h, and n_h is the number of PSUs selected for the sample in stratum h.

The first-stage variance estimator (disregarding the second-stage) is defined as:

$$\widehat{\text{VAR}}(\widehat{\mu}_h) = \frac{1}{n_h(n_h - 1)} \sum_{i=1}^{n_h} (\overline{y}_{hi} - \widehat{\mu}_h)^2$$
(4)

For the model-assisted scenario, we implemented case A two-stage estimators (Särndal et al., 1992). The estimator of the population mean consists of the sum of a prediction-based term and a residual-based adjustment term that reflects the sampling design (Eq. (5)). For wall-to-wall auxiliary data, the prediction-based term is the synthetic estimator ($\hat{\mu}_h$ syn) calculated as the mean of calibrated map predictions (\hat{y}_{hg}) over all PSUs within the population (g) in stratum h (Särndal et al., 1992, p. 399), which in this case corresponds to AGB means over the 4 × 4, 5 × 5 or 2 × 2 map units from our country-calibrated maps (Eq. (1)). The within-stratum adjustment term (ε_{hi}) is computed as the difference between the AGB mean observations over the plots within the selected i^{th} PSU (\hat{y}_{hi}), and their corresponding mean model prediction for the i^{th} PSU (\hat{y}_{hi}), $\varepsilon_{hi} = \bar{y}_{hi} - \hat{y}_{hi}$. For a model calibrated at the level of PSUs, the estimator is (Lohr, 2010; McRoberts et al., 2022):

$$\widehat{\mu}_h = \frac{1}{N_h} \sum_{q=1}^{N_h} \widehat{y}_{hg} + \frac{1}{n_h} \sum_{i=1}^{n_h} \varepsilon_{hi}$$
(5)

where N_h is the number of first-stage population units in stratum h.

The model-assisted variance estimator is the two-stage variance estimator, assuming the second-stage component of the variance to be negligible, equivalent to (Málaga et al., 2022) with observations replaced by model prediction residuals. It accommodates the influence of the field-based PSU being a mean over plots within the PSU. For N_h

large and $n_h \ll N_h$, the estimator can be approximated by:

$$\widehat{\text{VAR}}(\widehat{\mu}_h) = \frac{1}{n_h(n_h - 1)} \sum_{i=1}^{n_h} (\varepsilon_{hi} - \overline{\varepsilon_h})^2$$
(6)

where $\overline{\varepsilon_h} = \frac{1}{n_h} \sum_{i=1}^{n_h} \varepsilon_{hi}$.

2.5.2. Tanzania

The field-based baseline scenario estimators in Tanzania resemble those of the previous countries. Like in Peru and Mozambique, we assume that the clusters are selected by simple random sampling. An overestimation of the variance is a plausible consequence of ignoring the original systematic design (Næsset et al., 2020). We estimated stratumwise means and variances applying the simple expansion estimators of Eqs. (3) and (4), respectively.

In our model-assisted scenario, we followed case B two-stage estimators (Särndal et al., 1992, p. 323; McRoberts et al., 2024). Similar to Eq. (5), the estimator for the mean comprises a prediction-based term and a residual-based adjustment term (Eq. (7)). While the estimators may appear similar, the key distinction lies in the spatial support (the domain informed by a certain value, Kyriakidis, 2004) on which the analysis is conducted. In Eq. (7), the within-stratum synthetic estimator $(\hat{\mu}_h \, syn)$ is calculated as the average AGB predicted values for all map units. These predictions encompass the individual map units predicted from the calibrated map, \hat{y}_{hg} , as obtained from Eq. (2). Consistently, the within-stratum adjustment term is computed as the difference between the AGB observation for the j^{th} plot in the i^{th} PSU (y_{ij}) , and the corresponding AGB model prediction for the jth biomass map unit in the ith PSU (\hat{y}_{hij}) derived from Eq. (2), $\varepsilon_{ij} = y_{ij} - \hat{y}_{ij}$. For two-stage sampling designs and a model calibrated between plots and CCI individual map units (Särndal et al., 1992, p. 323), the estimator is defined as:

$$\widehat{\mu}_h = \frac{1}{N_h} \sum_{n=1}^{N_h} \widehat{y}_{hg} + \frac{1}{n_h} \sum_{i=1}^{n_h} \overline{\varepsilon}_{hi}$$
(7)

where $\overline{\varepsilon}_{hi} = \frac{1}{m_{hi}} \sum_{j=1}^{m_{hi}} \varepsilon_{hij}$, m_{hi} is the number of plots within the i^{th} PSU, N_h is the number of map units in stratum h, and n_h is the number of PSUs selected for the sample in stratum h.

With the finite population correction term $\left(1-\frac{n_h}{N_h}\right)\approx 1$; and considering the second-stage component of the variance to be negligible, the variance estimator reduces to (Särndal et al., 1992, p. 325; McRoberts et al., 2024):

$$\widehat{\text{VAR}}(\widehat{\mu}_h) = \frac{1}{n_h(n_h - 1)} \sum_{i=1}^{n_h} (\overline{\varepsilon}_{hi} - \overline{\overline{\varepsilon}}_h)^2$$
(8)

where $\overline{\overline{\varepsilon}}_h = \frac{1}{n_h} \sum_{i=1}^{n_h} \overline{\varepsilon}_{hi}$

2.5.3. Guyana

For Guyana, we accounted for the original proportions of the stratum of interest within the $10\ km\times 10\ km$ grid cell, which were introduced as weights into the first-stage estimators of the mean and variance, equivalently to eq. 5.28 Lohr (2010, Section 5.3). Hence, the stratified estimator of the population mean for our field-based scenario is expressed as:

$$\widehat{\mu}_h = \frac{\sum_{i=1}^{n_h} w_{hi} \, \overline{y}_{hi}}{\sum_{i=1}^{n_h} w_{hi}} \tag{9}$$

where h refers to the stratum, $\bar{y}_{hi} = \frac{1}{m_{hi}} \sum_{j=1}^{m_{hi}} y_{hij}$, y_{hij} is the AGB observation for the j^{th} plot in the i^{th} PSU, m_{hi} denotes the number of plots within the i^{th} PSU, n_h is the number of PSUs selected for the sample in

stratum h, and w_{hi} is the area proportion of stratum h in a 10 km \times 10 km cell, i.e. $w_{hi} = \frac{\text{area of stratum } h \text{ in } 10 \text{ km x } 10 \text{ km grid cell}}{\text{area a } 10 \text{ km x } 10 \text{ km grid cell}}$.

Considering the finite population correction terms $\left(1-\frac{n_h}{N_h}\right)\approx 1$, and the second-stage component of the variance negligible, the estimator of the variance of the field-based scenario is:

$$\widehat{\text{VAR}}(\widehat{\mu}_h) = \frac{1}{\overline{w_h}^2} \begin{bmatrix} \sum_{i=1}^{n_h} (w_{hi} \, \overline{y}_{hi} - w_{hi} \, \widehat{\mu}_h)^2 \\ n_h(n_h - 1) \end{bmatrix}$$
(10)

where additionally, $\overline{w_h}$ is the average weight (w_{hi}) within the stratum of interest.

Like in Tanzania, for our model-assisted scenario, we followed case B two-stage estimators (Särndal et al., 1992, p. 325; McRoberts et al., 2024). Similar to Eq. (7), the estimator of the mean compromises the synthetic estimator ($\hat{\mu}_h$ syn), which encompasses all individual map unit predictions of the calibrated map (\hat{y}_{hg}) obtained from Eq. (2), and a residual-based adjustment term (Eq. (11)). An adaption to Eq. (7) is the incorporation of the proportion of the h stratum of interest within the original $10 \text{ km} \times 10 \text{ km}$ grid cell (w_{hi}) within the adjustment term. The model-assisted estimator of the mean is defined as:

$$\widehat{\mu}_{h} = \frac{1}{N_{h}} \sum_{p=1}^{N_{h}} \widehat{y}_{hg} + \frac{\sum_{i=1}^{n_{h}} w_{hi} \, \overline{\varepsilon}_{hi}}{\sum_{i=1}^{n_{h}} w_{hi}}$$
(11)

where $\overline{\varepsilon}_{hi} = \frac{1}{m_{hi}} \sum_{j=1}^{m_{hi}} \varepsilon_{hij}$ and N_h is the number of map units in stratum h.

Considering the finite population correction terms $\left(1-\frac{n_h}{N_h}\right)\approx 1$, and the second-stage component of the variance negligible, the estimator of the variance of the model-assisted scenario is reduced to:

$$\widehat{\text{VAR}}(\widehat{\mu}_h) = \frac{1}{\overline{w_h^2}} \begin{bmatrix} \sum_{i=1}^{n_h} (w_{hi} \ \overline{\varepsilon}_{hi} - w_{hi} \ \overline{\overline{\varepsilon}}_h)^2 \\ n_h(n_h - 1) \end{bmatrix}$$
(12)

where
$$\overline{\overline{\varepsilon}}_h = \frac{\sum_{i=1}^{n_h} w_{hi} \overline{\varepsilon}_{hi}}{\sum_{i=1}^{n_h} w_{hi}}$$
.

2.5.4. Country estimates

We used stratified estimators for our country-wise estimates (Næsset et al., 2020):

$$\widehat{\mu} = \sum_{h=1}^{H} \frac{N_h}{N} \ \widehat{\mu}_h \tag{13}$$

$$\widehat{\text{VAR}}(\widehat{\mu}) = \sum_{h=1}^{H} \left(\frac{N_h}{N}\right)^2 \widehat{\text{VAR}}(\widehat{\mu}_h)$$
(14)

In Peru and Mozambique, N_h represents the number of all PSUs within the population in stratum h (Eq. (5)); whereas in Tanzania and Guyana N_h refers to all individual map units in stratum h (Eqs. (7) and (11), respectively). Further, N refers to the country-wise sum of N_h . N in Peru is equivalent to 1,673,270, in Mozambique to 253,643,899, in Tanzania to 1,262,897,847 and Guyana to 20,012,861.

2.5.5. Relative efficiency

As in Málaga et al. (2022), we assessed the contribution of the biomass map to increase the precision of (sub)national AGB estimates by means of relative efficiency (RE) which compares the variance estimate for our field-based scenario, $\widehat{\text{VAR}}(\widehat{\mu}_h)_{\text{field-based}}$, relative to the model-assisted variance estimate, $(\widehat{\text{VAR}}(\widehat{\mu}_h)_{\text{map}})$.

$$RE = \frac{\widehat{VAR}(\widehat{\mu}_h)_{field-based}}{\widehat{VAR}(\widehat{\mu}_h)_{map}}$$
 (15)

3. Results

3.1. Field-based and model-assisted AGB estimates

We assessed the performance of the CCI biomass map products (v4) in four country case-studies. Our findings indicate that, prior to calibration, the CCI biomass maps systematically underestimate aboveground biomass (AGB) at both country and stratum levels in three of the four country case-studies. Within the four strata in the Peruvian Amazonia, we observed no systematic error between the 2017 CCI biomass synthetic map estimates and the field-based AGB estimates (Fig. 2, supporting systematic error analysis in Appendix C). In contrast, towards the north-eastern side of the Amazon basin, synthetic estimates from the map consistently underestimated the stratum-wise AGB values when compared to those obtained from the Guyana NFI data (Fig. 2 and Appendix C). Among smaller biomass biomes in East African countries, the CCI products almost consistently underestimated stratum-wise NFI AGB estimates in Tanzania (with exception of strata 13, 15 and 18) and Mozambique (Fig. 2 and Appendix C).

After fitting linear regression models to locally calibrate the remote-sensing-based products we found consistent, relatively weak coefficients of determination ($\rm R^2$ 0.01–0.39) in all countries, with some regression model relationships being non-significant (p>0.05) (Table 2). There was no evident trend in the level of agreement between map and field-based units across large or small biomass biomes, nor at the level at which the regression models associating map and field-based units were constructed (Fig. 3). At both large and small biomass, the model-assisted estimates exhibited little agreement with field-based estimates at the local level (Appendix D displays map-to-plot relationships in more detail). Non-intercept models were used in the HZ stratum of Peru and stratum 18 in Tanzania to avoid calibrating to unrealistic negative AGB values. Some specific strata in Tanzania and Mozambique incorporated heteroscedasticity correction in the regression models (Table 2).

In general, after calibrating the biomass map with country-specific NFI data, the model-assisted stratum-wise and country-level AGB estimates were found to be well-aligned with the corresponding field-based estimates (Fig. 2, Table 2). Within the Peruvian Amazon, the modelassisted stratum-wise AGB estimates were in the range of $163.5-254.2 \text{ Mg ha}^{-1}$, with an overall estimate of 219.5 Mg ha⁻¹. Similarly, in Guyana, the model-assisted mean estimates (321.5 to 574.4 Mg ha⁻¹) were in a similar order as those from the NFI. Likewise, in Tanzania, the model-assisted mean estimates were in the order $10.4-106.5 \text{ Mg ha}^{-1}$ and 42.7 Mg ha^{-1} , at the stratum and country level, respectively. In Mozambique, the model-assisted estimates ranged between 43.6 and 85.6 Mg ha⁻¹ among strata and 58.0 Mg ha⁻¹ at the country level. However, significant differences were found between field-based and model-assisted AGB estimates in the semi-deciduous forest (SDF) and semi-evergreen forest (SEF) strata in Mozambique, as well as at the country level. Fig. E.1 in Appendix E provides a visual representation of the uncalibrated and calibrated versions of the CCI biomass maps for the four country case studies.

3.2. Contribution of the map to the precision of (sub)national estimates

We evaluated the gain in precision of model-assisted (sub)national AGB estimates compared to field-based estimates across countries with diverse biomass densities, NFI sampling designs, and plot configurations. Our findings demonstrate that introducing a locally calibrated biomass map as a source of auxiliary information to the conventional NFI information fairly improved the precision of stratum and countrywise AGB estimates. The degree of improvement is expressed by

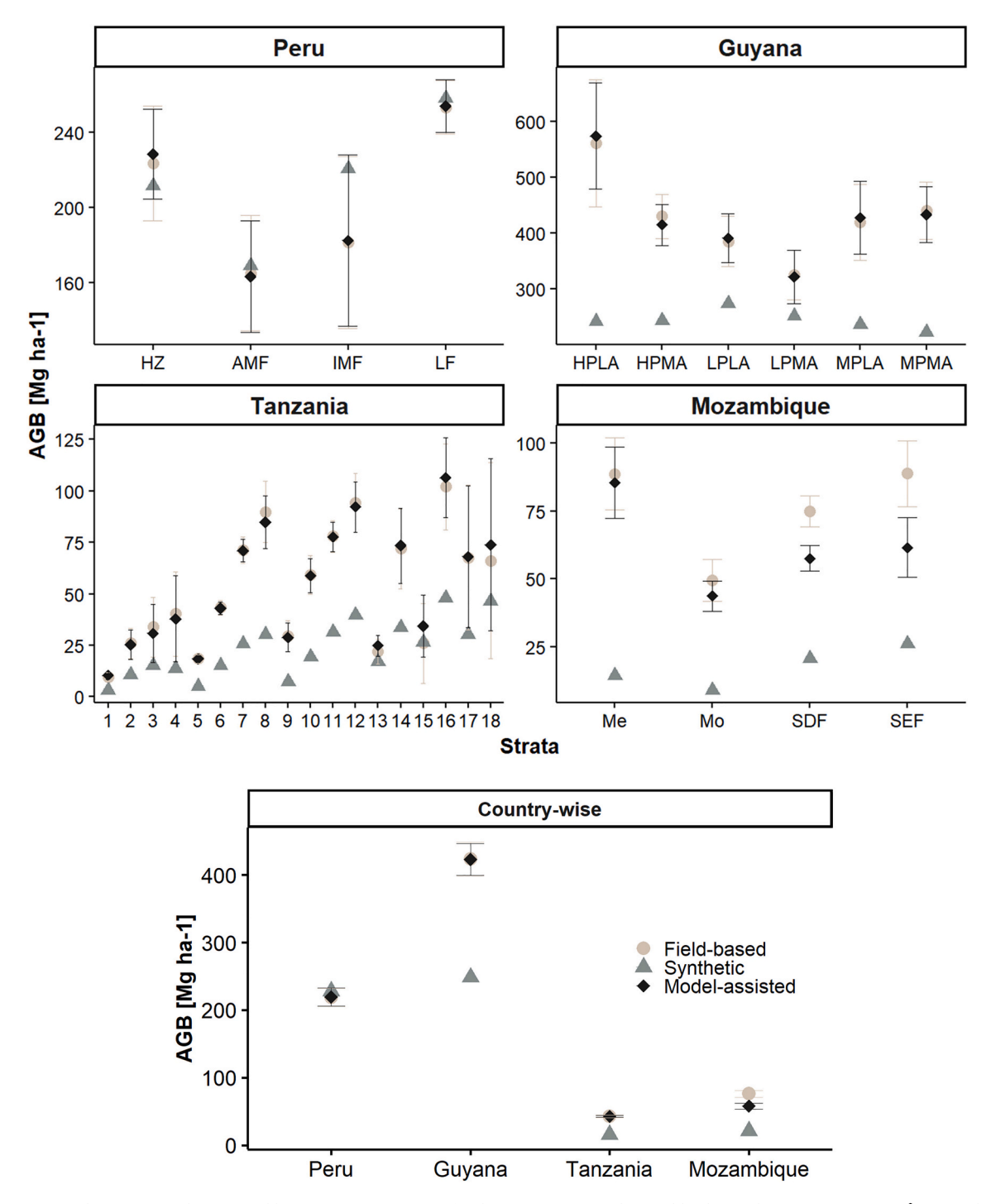


Fig. 2. Per stratum and per country aboveground biomass (AGB) estimates for the country case-studies. Unlike the synthetic mean estimate ($\hat{\mu}_h$ syn, indicated by \triangle), the field-based (\blacklozenge) and model-assisted (\blacksquare) mean estimates are accompanied by their 95 % confidence intervals.

means of RE (Eq. (15)), where values >1.0 indicate a gain in precision (smaller variance) (McRoberts et al., 2014). For instance, an RE value of 1.2 corresponds to a 20 % increase in precision. In Peru, the gain in precision was in the order of 0–60 %. For Tanzania and Mozambique, the contribution to precision at the stratum and country levels was slightly greater, ranging from 0 to 70 % and 0 to 100 %, respectively. The smallest gain in precision through locally calibrating the global biomass map was observed in Guyana (Table 2). Although no clear trend was evident between the gain in precision and the magnitude of biomass density (Fig. 3), at the country level, the gain in precision was slightly greater among small biomass (RE of 1.5 in Mozambique and 1.3 in

Tanzania) compared to large biomass biomes (RE of 1.1 in both Peru and Guyana). In general, stronger map-to-plot correlations result in greater RE values (Fig. 3).

4. Discussion

Following the results, the discussion section delves deeper into our model-assisted AGB estimates compared to the field-based ones, examines the gains in precision from our model-assisted estimates, and addresses the main takeaways from our four country case studies regarding the integration of global biomass maps with NFI data within the model-

Table 2
Field-based and model-assisted AGB estimates and the relative efficiency (RE) of the biomass map to increase the precision of the (sub)national AGB estimates.

Stratum n	n	Field-based		Model-assisted						RE
	$\widehat{\mu}$	$\widehat{\mathrm{VAR}}(\widehat{\mu})$	$\widehat{\mu}_{syn}$	model		R^2	$\widehat{\mu}$	$\widehat{\mathrm{VAR}}(\widehat{\mu})$		
Peru										
HZ	32	223.8	242.0	211.7	$\overline{y}_i{=}1.1\widehat{y}_i$	*	0.39	228.6	149.4	1.6
AMF	46	165.3	247.5	169.3	\overline{y}_i =93.4 + 0.4 \hat{y}_i		0.08	163.5	226.8	1.1
IMF	11	181.5	547.8	220.9	$\overline{\mathbf{y}}_i = 219.9 - 0.2 \widehat{\mathbf{y}}_i$		0.01	182.6	542.0	1.0
LF	210	253.5	52.0	258.2	\overline{y}_i =167.6 + 0.3 \hat{y}_i	*	0.02	254.2	50.8	1.0
Country	299	218.6	47.9	228.0	-		-	219.5	44.9	1.1
Mozambique										
Mecrusse	50	88.7	45.7	14.4	$\overline{y}_i = 78 + 0.5 \hat{y}_i$		0.01	85.6	45.1	1.0
Mopane	105	49.4	15.8	9.0	$\overline{y}_i = 30.3 + 1.4 \hat{y}_i \lozenge$	*	0.24	43.6	8.0	2.0
SDF	446	75.0	8.5	20.7	\overline{y}_i =21.5 + 1.8 \hat{y}_i \Diamond	*	0.17	57.5	5.8	1.5
SEF	120	88.8	38.2	26.1	$\overline{y}_i = 11.6 + 2.5 \hat{y}_i \lozenge$	*	0.23	61.6	31.2	1.2
Country	721	76.2	6.7	21.0	-		-	58.0	4.6	1.5
Tanzania										
1	241	9.6	1.1	3.3	y_{ij} =5.9 + 1.4 \hat{y}_{ij} \Diamond	*	0.01	10.4	0.9	1.3
2	69	26.0	13.6	10.7	$y_{ij} = 13.6 + 1.1 \hat{y}_{ij}$	*	0.03	25.4	13.1	1.0
3	27	33.9	55.9	15.1	$y_{ii}=9.3+1.6\widehat{y}_{ii}$	*	0.05	30.9	51.4	1.1
4	19	40.3	110.7	13.9	$y_{ii}=34.9+0.3\widehat{y}_{ii}$		0.01	38.0	113.5	1.0
5	678	18.6	1.1	5.1	$y_{ij}=9+2\hat{y}_{ij}$ \Diamond	*	0.05	18.5	0.8	1.4
6	641	43.4	3.3	15.1	$y_{ij}=13.6+2\hat{y}_{ij}$ \Diamond	*	0.13	43.1	2.3	1.4
7	467	71.4	10.3	25.9	$y_{ij}=14.6+2.2\hat{y}_{ij}$ \Diamond	*	0.15	71.1	7.8	1.3
8	159	90.0	57.8	30.2	$y_{ij} = 14.0 + 2.2 y_{ij} \lor y_{ii} = 7.6 + 2.7 \hat{y}_{ii} \diamondsuit$	*	0.13	84.8	43.3	1.3
9	98	29.4	15.0	7.4	$y_{ij}=7.0 + 2.7y_{ij} \diamondsuit$ $y_{ii}=19 + 1.4\hat{y}_{ii}$	*	0.21	28.9	12.3	1.2
10	162	59.3	23.3	19.3	.,	*	0.00	58.9	18.4	1.3
					$y_{ij}=20.3+2.1\hat{y}_{ij}$	*				
11	151	78.0	15.1	31.5	$y_{ij}=24.8+1.8\widehat{y}_{ij}$	*	0.12	77.8	13.2	1.1
12	85	94.3	52.1	39.5	$y_{ij}=24.6+1.8\hat{y}_{ij}$		0.21	92.3	39.3	1.3
13	103	22.1	9.2	17.2	$y_{ij}=7+1\widehat{y}_{ij}$	*	0.09	25.0	6.9	1.3
14	157	71.9	99.4	33.5	$y_{ij}=9.2+1.9\hat{y}_{ij}$	*	0.08	73.6	86.7	1.1
15	8	26.0	99.1	26.5	$y_{ij} = 14.8 + 0.7 \hat{y}_{ij}$		0.16	34.4	59.9	1.7
16	100	102.0	113.8	47.9	$y_{ij} = 14.6 + 1.9 \hat{y}_{ij}$	*	0.08	106.5	97.0	1.2
17	30	67.8	324.4	30.4	y_{ij} =35.4 + 0.8 \hat{y}_{ij}	*	0.03	68.2	308.0	1.1
18	13	66.1	590.5	46.6	$y_{ij}=1.6\widehat{y}_{ij}$	*	0.21	73.8	453.8	1.3
Country	3208	42.8	0.8	15.6	-		-	42.7	0.6	1.3
Guyana										
HPfc/LA	8	561.4	3351.6	241.3	$y_{ij} = 652.2 - 0.6 \hat{y}_{ij}$		0.06	574.4	2334.0	1.4
HPfc/MA	35	430.2	414.7	242.5	$y_{ij} = 289.3 + 0.5\hat{y}_{ij}$	*	0.06	414.7	363.5	1.1
LPfc/LA	11	385.3	532.9	273.1	$y_{ij} = 516 - 0.5\hat{y}_{ij}$		0.06	391.2	509.4	1.0
LPfc/MA	20	324.9	521.0	250.8	$y_{ii} = 276.7 + 0.2\hat{y}_{ii}$		0.02	321.5	603.6	0.9
MPfc/LA	18	419.8	1205.7	235.8	$y_{ii} = 300.2 + 0.6 \hat{y}_{ii}$		0.04	427.4	1107.9	1.1
MPfc/MA	25	439.8	688.3	222.7	$y_{ij} = 372.5 + 0.3 \hat{y}_{ij}$		0.02	433.5	658.0	1.0
Country	117	423.6	163.3	248.5			_	422.9	145.8	1.1

Where: $\hat{\mu}_{syn}$ corresponds to the uncalibrated version of the map; \Diamond to strata in which models were corrected for heteroscedasticity; and * to strata where the models were significant (p < 0.05). Models are expressed in terms of Eqs. (1) and (2).

assisted estimation framework.

4.1. Field-based and model-assisted AGB estimates

Both our field-based and model-assisted AGB estimates show reasonable alignment with official reports from the respective countries. Our Peruvian Amazon estimates are fairly similar to those described in a SERFOR (2020) report (AMF: 145.4 Mg ha⁻¹; IMF: 166.5 Mg ha⁻¹; LF: 295.4 Mg ha⁻¹; HZ:188.6 Mg ha⁻¹). In Mozambique, with the exception of the SDF stratum, both country and stratum-wise AGB estimates aligned similarly to those described on the country's REDD+ Forest Reference Emission Level (Mopane: 40.7–48.4 Mg ha⁻¹; Mecrusse 73.2–84.1 Mg ha⁻¹; and SEF: 94–105.8 Mg ha⁻¹) (Government of Mozambique, 2018). In Tanzania, although expressed in different classes, our AGB estimates are in line with those described in a NAFORMA report (ranging from 2.9 in open lands to 59.5 Mg ha-1 in forested areas) (MNRT, 2015). Finally, in Guyana, there are no significant differences

between our AGB estimates and those reported in the REDD+ Reference Level (HPfc/MA: 395.1 Mg ha $^{-1}$; HPfc/LA; 546.1 Mg ha $^{-1}$, and MPfc/MA and MPfc/LA: 468.78 Mg ha $^{-1}$) (Government of the Cooperative Republic of Guyana, 2015). Differences between our findings and official reports may arise from the assumptions made in our study, such as population definition and the challenges encountered during map-to-plot harmonization, as discussed in Section 4.3.

Our study sheds light on the limitations of the CCI biomass map products (v4) in accurately predicting AGB and underscores the importance of using local reference data to calibrate the global products for achieving accurate (sub)national estimates. With the exception of Peru, the uncalibrated form of the maps systematically underestimated AGB at the (sub)national level in both large and small biomass biomes. Málaga et al. (2022) showed systematic overestimation of the 2017 CCI biomass product (v3) within the Peruvian Amazon, whereas this systematic error is absent in v4. Notably, AGB densities within the Guyana shield have been reported to be twice as large as within the Western

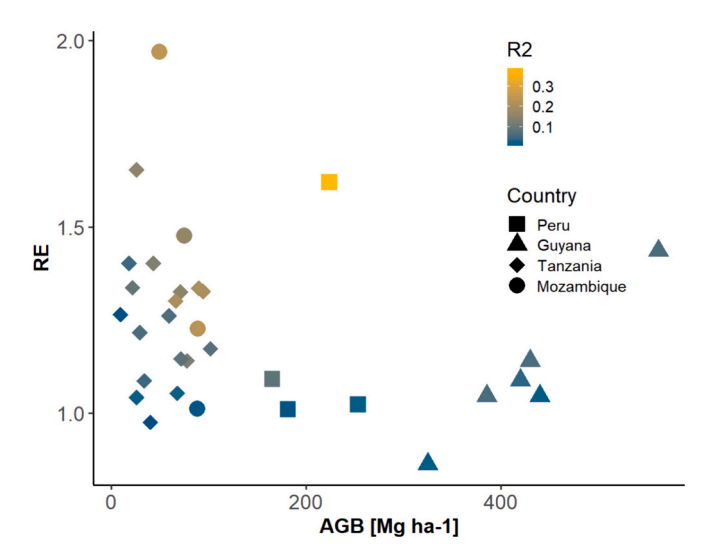


Fig. 3. Stratum-wise field-based mean above ground biomass (AGB) estimates and correspondent relative efficiencies (RE), colored in terms of regression model $\rm R^2$.

Amazon, mostly attributed to taller trees found in the former region (Feldpausch et al., 2012), which likely contributes to the substantial underestimation by v4 in Guyana. Furthermore, differences might be partially explained by the reference data of Guyana's NFI including trees starting at 5 cm DBH, whereas the biomass map does not fully represent biomass in the understory. Hunka et al. (2023) found overall fair agreement between the uncalibrated CCI biomass map (v4) mean AGB estimates and (sub)national NFI-based estimates in Peru, Mexico, Laos, and Spain. They reported that approximately half the time, the map produced estimates falling within the 95 % confidence interval of country NFI-based estimates. In a different study, Næsset et al. (2020) applied a prior version of the product used in our research within a smaller study area in Tanzania and reported no systematic under- or overestimation of the map when compared to local reference data. Conversely, our results do signal the need of calibrating the global product for producing accurate (sub)national synthetic AGB estimates. However, as global biomass products continue to enhance—as exemplified by the improvement from v3 to v4 in the Peruvian Amazon—we can envision a future where achieving accurate (sub)national AGB synthetic estimates becomes a common practice in large and small biomass settings.

A crucial insight gained from the calibration was the limited alignment between the NFI reference data and the map values at the smallest spatial support level, whether it was among ~100 m CCI map units (i.e. Guyana and Tanzania) or polygons of aggregated map units (\sim 400–500 m in Peru and $\sim\!200$ m in Mozambique). Regardless of large or small biomass regions, the coefficients of determination were uniformly small. Even within the Peruvian Amazon, where the stratum-wise synthetic AGB map estimates mirrored those based on NFI information, the relationship at the local level was still weak. The absence of agreement at the finest spatial support level is not surprising, as previous studies have likewise reported weak coefficients of determination between global remote sensing-based products and local reference data, with values of $R^2 < 0.3$ (Réjou-Méchain et al., 2019) and $R^2 < 0.4$ in Tanzania (Næsset et al., 2020). Similarly, a study comparing CCI biomass change estimates with reference data at global scale indicated that NFI-based estimates showed only a moderate level of agreement with the global product (R² ~ 0.2) starting at 1 km aggregation (Araza et al., 2023).

4.2. Using global biomass maps to increase the precision of (sub)national AGB estimates

The introduction of CCI biomass maps, calibrated with local regression models, as a source of auxiliary information resulted in a fair increase in precision of our (sub)national AGB estimates. From a previous study within the Peruvian Amazon, we showed that transitioning from a locally calibrated 2017 v3 product (RE = 1.0-1.5) (Málaga et al., 2022), to the v4, resulted in marginal improvements in precision for certain strata while causing a decline in others. A study conducted in Tanzania reported a notably larger contribution from a preceding locally calibrated 2010 GlobBiomass map (Santoro et al., 2018), to the precision of field-based estimates (RE = 2.7) (Næsset et al., 2020). Still, given the different extent of the study and reference data (evidenced, among other factors, by differing sample sizes and site re-measurements), direct comparisons must be interpreted with caution. In the LPfC/MA stratum of Guyana, an increase in variance from our model-assisted estimates is observed (RE < 1), which may be attributed to the aggregation or weighting effect. The modest contribution of the biomass maps to increasing the precision of model-assisted (sub)national AGB estimates can be attributed to the weak map-to-plot correlations at the finest spatial scale observed across biomes. The factors contributing to weak map-to-plot agreement are manyfold and can be attributed to the limitations of the remote-sensing-based global biomass products (i.e., in capturing fine scale AGB variability), the limitations of the reference data (i.e., AGB measurement errors, positional errors), the way these two sources of information are integrated (i.e., mismatches in the spatial support of the remote sensing-based information and the size of the reference data), along with the chosen inferential approach. All of which are addressed in more detail in Section 4.3.

Notwithstanding, even a small gain in precision can entail nonmarginal advantages. In the case of simple random sampling of the clusters and the number of plots within a cluster remaining constant, an initial sample size of 91 clusters within the HZ stratum in Peru and a RE of 1.6 implies that the same targeted precision could be achieved with a reduced number of clusters (~60) by incorporating the calibrated map as auxiliary data (cf. McRoberts et al., 2014). Achieving precision goals with a smaller sample size is particularly advantageous for countries like Peru, navigating the challenges of completing their first ever NFI. Yet, it's vital to ensure that reducing the sample size for country-level AGB estimation does not risk the precision of other attributes measured in a country's NFI (i.e., biodiversity and other forest structural parameters), as well as safeguard the representativeness of forest ecosystems vet encompassed within the evaluated sampling units. Furthermore, for countries that have concluded their initial NFI rounds (e.g., Tanzania, Mozambique, Guyana), the incorporation of a locally calibrated global map translates into greater confidence in AGB estimates, reflected by narrower confidence intervals in their country-level greenhouse gas (GHG) reporting. Reducing uncertainties as far as practical in country GHG inventories is an IPCC good practice guideline under the UNFCCC (Eggleston et al., 2006, Vol 1, Chap 1, Section 1.2). Similarly, in REDD+ results-based payment frameworks like the Forest Carbon Partnership Facility (FCPC), in which all of these countries participate, the estimation and reduction of uncertainties related to emission factors is encouraged. This holds particular significance since it translates into incentives, emphasizing how countries stand to gain from improved precision and narrower confidence intervals given the encouraged conservative approach when establishing reference levels (FCPF, 2020). Finally, Tanzania, Guyana and Mozambique have yet to update their field campaigns, meaning that among countries struggling with updating their NFIs, further studies are merited for exploring the opportunities global biomass products present for efficiently planning future field campaigns, potentially involving less intensive sampling.

A recent study conducted in Paraguay, comparing hybrid inference AGB estimates based on a country-specific GEDI-calibrated model, yielded a boost in precision compared to AGB estimates based on the country's NFI data (Bullock et al., 2023). The substantial increase in precision could be related to the better agreement found between the predicted GEDI values and reference data, along with the substantial increase in sample size achieved through the use of GEDI shots to estimate sampling variability in hybrid inference. Nonetheless, the focus of our study is on model-assisted estimation, maintaining the unbiased or nearly unbiased nature of design-based inference (McRoberts et al., 2014). The selection of unbiased estimators aligns with an IPCC good practice guideline, urging countries to neither over- nor under-estimate GHG emissions or removals as far as can be judged (Eggleston et al., 2006; Næsset et al., 2020).

4.3. Map-to-plot harmonization takeaways that countries face when integrating global biomass products with NFI data

The integration of remote sensing-based products with NFI data introduces a fresh set of challenges within the model-assisted estimation framework, given that NFIs were not initially designed to accommodate remote sensing-based products. A key take-away from our four country case-study within the tropics is that no single recipe fits all circumstances. The selection of the estimators under model-assisted inference requires a context-specific assessment that accommodates the decisions made by the countries in the design and implementation of the NFIs. Notwithstanding, common lessons learned emerged from the integration of global biomass map with NFI data in the model assisted-estimation framework. These insights will now be elaborated and exemplified in light of the unique characteristics of each country's NFI.

The NFI sampling design determines the selection of the specific model-assisted estimator. While variations are inherent among the NFIs of these four countries, a shared characteristic —widespread among other tropical countries— is the adoption of clustered plots following some kind of fixed configuration within the cluster (Nesha et al., 2022). In Tanzania, the inverse L-shaped cluster configuration adheres to a fully fixed systematic design. In Peru, the allocation of the anchor point of the L-shaped cluster is random, while the orientation remains fixed. In Guyana, both the anchor point and orientation of the L-shaped plots are randomized within a larger grid cell. In Mozambique, the cluster is arranged in the form of a fixed squared. Clusters are often employed in NFIs to enhance logistical efficiency, owing to the considerable effort required to access sample plots (Tomppo et al., 2010). However, methods for accommodating cluster designs with remote sensing-based products under a model-assisted estimation framework have not been extensively explored. For this purpose, our study embraced two-stage model-assisted estimators, as outlined by Särndal et al. (1992, pp. 304-305) and elaborated by McRoberts et al. (2024). This approach considers the distance among plots within the same cluster relative to the size of the map units as a defining criterion to distinguish between case A (involving some level of aggregation) and case B (element sampling). When two or more plots may fall within the a single biomass map unit (~100 m, e.g. Peru and Mozambique) the expected 1:1 relationship between map units and plots is disrupted Särndal et al. (1992); with potentially unknown implications for the estimated variance. Implementing case B across countries could be possible if resampling the map into smaller units similar in size to the plots or distance between subplots, thereby maintaining the 1:1 relationship. However, this approach might entail more processing capacity and not necessarily produce more precise results, as evidenced by the already modest level of map-to-plot agreement at approximately 100 m resolution.

For full consistency across field-based and model-assisted estimates, in case of a stratified sampling design, the stratification layer should completely cover the country's defined population and it should be consistent with the NFI's sampling design. Peru stratified the country into six strata defined by different criteria that are expressed in a map, four of which were part of this study (MINAGRI and MINAM, 2016). Mozambique employed a relatively coarse stratification map that exhibited disparities between map vegetation classes and on-ground

conditions and resulted in the re-location of field-samples (Alegria, 2020). Tanzania initially followed a double sampling for stratification design, which was here reduced to a single-phase design by adopting a stratification layer produced later that mirrored the original criteria (Næsset et al., 2020). Guyana's stratification is rooted in accessibility considerations, which underwent modifications during its implementation (Petrova et al., 2013). While the study's best interest rested on ensuring consistent cross-scenario estimates, the assumptions made around the stratification reveal consequences. For instance, in Mozambique, discrepancies observed between our field-based and model-assisted AGB mean estimates (both at the country level and within the SDF and SEF strata), may be attributed to the potential lack of representation of the reference data to capture the within-strata variability, possibly influenced by the decision to relocate some of the plots during the implementation of the NFI. Despite the country's implementation of alternative strategies to account for NFI deviations (Government of Mozambique, 2018), for the purposes of this study we were constrained to employ the original stratification layer and assume its representativeness in terms of the original inclusion probabilities.

A forest mask may be needed to properly reflect how the population is defined by the country's NFI. In Peru, a country-specific forest mask needed to be introduced because the biomass maps provide spatially-continuous AGB estimates, whereas the NFI AGB estimates are confined to forested sites. Tanzania's field-crew measurements encompassed trees meeting the minimum DBH threshold, regardless of their location in or outside forested sites (MNRT, 2015), hence no forest masking was necessary. In the case of Guyana, the stratification layer inherently adjusted for forest cover (Petrova et al., 2013); and the same was assumed for Mozambique.

CCI map epochs were selected to closely align with the countries' NFI implementation timeframe so as to reduce potential uncertainties related to temporal mismatches (Duncanson et al., 2021). While the implementation periods for Mozambique and Tanzania were restricted to 3-4 years, countries within the Amazon opted for a longer implementation timeframe in stages. Moreover, the progress of Peru's NFI to date is around 30 % and is being carried out through panels which represent uniformly distributed sample units across each stratum. As the NFI in Peru remains ongoing, such panel implementation holds implications to the estimator. Hence, as implemented in a previous study, we confined our analysis to the panels (sections) of the Peruvian Amazon where progress has been made (Málaga et al., 2022). Discrepancies between the AGB means estimated in our study and those reported in the country's official reports (SERFOR, 2020) might stem from the assumptions made when defining the population and its effects in a slightly smaller the sample size.

Additional considerations regarding the selected two-stage estimator. The employed variance estimators for two-stage sampling assume random selection of both PSUs and SSUs within PSUs. However, within the four countries assed in this study, the SSUs are arranged in various fixed spatial configurations. It's prudent to acknowledge that disregarding the actual fixed spatial layout of plots might carry unforeseen consequences for the variance estimation. Furthermore, a notable aspect involving the two-stage model-assisted estimators used in this research is that, from a design-based perspective, we found the contribution of the within PSU variability (second component of the variance) to be negligible in comparison to the among PSU variability (first-stage).

To further increase the precision of AGB estimates within the model-assisted framework, we need better agreement of the map-to-plot relationship, particularly at finer scales. This entails enhancement of the remote sensing-based products' ability to predict local AGB variability and to reduce uncertainties associated with integrating the two sources of information. Næsset et al. (2016) observed a threefold augmentation in the precision of AGB estimates upon transitioning from coarser resolution remotely sensed data to finer resolution data (such as ALS or Rapid Eye) in miombo woodlands. At present, to mitigate local

restrictions inherent to coarse-scale remote sensing-based biomass products, the adoption of finer resolution information may be considered. However, such decision rests upon individual countries, weighing the potential increase in precision against the financial cost and processing capacities associated with finer resolution power. Ultimately, the difference in the spatial support between global biomass maps and NFI field-plots has shown to be a relevant contributor to the sources of uncertainty when integrating map and field-based information (Málaga et al., 2022). Uncertainties arising from the spatial support mismatches between the two sources of information are more pronounced in areas with forests displaying greater AGB variability and in cases where field plots are particularly small (Réjou-Méchain et al., 2014). The influence of geo-location errors on model-assisted estimation has also been noted (Saarela et al., 2016), albeit to a lesser extent when the information is aggregated (Málaga et al., 2022), as we did in the cases of Peru and Mozambique. In broad terms, the magnitude of uncertainties arising from integrating remote sensing-based information and field data decrease as the spatial support of the map and field data become more similar in size and better overlap (Duncanson et al., 2021; Tomppo et al., 2017). Furthermore, from the use of remote sensing-based products as sources of auxiliary information, RE has also been seen to benefit (by 50 %) when the size of a plot doubles (200 m²-400 m²) (Næsset et al., 2015). Yet, determining the optimal NFI plot size and configuration for integration with remote sensing products involves a comprehensive discussion encompassing criteria such as efficiency, cost, and representativeness, among others; one that extends the scope of this study.

5. Conclusions

We conducted an evaluation of robust model-assisted estimation strategies, using CCI global biomass maps as a source of auxiliary information to increase (sub)national AGB precision across varying biomass densities and diverse NFI sampling designs. While country-specific characteristics involving the NFI objectives and sampling design guided tailored model-assisted inference strategies, common lessons emerged from integrating global biomass maps with NFI data within this framework.

Our four country analyses revealed that, while the uncalibrated CCI biomass maps (v4) tend to underestimate (sub)national AGB across biomes, after calibration, our model-assisted estimates aligned well with field-based estimates and country reports. Consequently, the use of global products for (sub)national estimates without prior calibration using local reference data would still not be recommended at this stage. Upon calibration, introducing the global maps as auxiliary information to (sub)national estimates resulted in a fair gain in precision; slightly larger within low biomass countries. The increase in precision holds promising benefits, including optimized NFI sampling intensities and greater confidence in AGB estimates for GHG reporting, aligning with IPCC good practice guidelines.

The prospect of achieving even greater precision relies on improving map-to-plot correlations at finer spatial scales. This improvement can be attained through more advanced remote sensing-based biomass products that better predict local AGB variability as well as accounting for and reducing the sources of uncertainties posed by integrating biomass maps with NFI reference data, especially related with the lack of agreement in their spatial support. As these factors improve, the potential for increasing the precision of AGB (sub)national estimates with the adaptable model-assisted framework here presented becomes even more prominent.

CRediT authorship contribution statement

Natalia Málaga: Original and revised draft, Visualization, Methodology, Formal analysis, Conceptualization, Writing – review & editing. **Sytze de Bruin:** Original and revised draft, Methodology, Conceptualization, Writing – review & editing. **Ronald E. McRoberts:** Original and

revised draft, Methodology, Writing – review & editing. Erik Næsset: Original and revised draft, Methodology, Writing – review & editing. Ricardo de la Cruz Paiva: Original and revised draft, Data curation. Alexs Arana Olivos: Original and revised draft, Data curation. Patricia Durán Montesinos: Original and revised draft, Data curation. Mahendra Baboolall: Original and revised draft, Data curation. Hercilo Sancho Carlos Odorico: Original and revised draft, Data curation. Muri Gonçalves Soares: Original and revised draft, Data curation. Sérgio Simão Joã: Original and revised draft, Data curation. Eliakimu Zahabu: Original and revised draft, Data curation. Dos Santos Silayo: Original and revised draft, Data curation. Martin Herold: Original and revised draft, Methodology, Funding acquisition, Conceptualization.

Declaration of competing interest

The authors declare that they have no known competing financial interests or personal relationships that could have appeared to influence the work reported in this paper.

Data availability

The authors do not have permission to share data.

Acknowledgements

The authors gratefully acknowledge support through the CCI Biomass Phase 2 project funded by ESA and the Transparent Monitoring project funded by the International Climate Initiative (IKI) of the German Federal Ministry of the Environment, Nature Conservation and Nuclear Safety (BMU) (Project number 20_III_108_Global_A_Transparent Monitoring Land Sector). Part of the research was supported by the Open-Earth-Monitor Cyberinfrastructure project that received funding from the European Union's Horizon Europe Research and Innovation Program under grant agreement No. 101059548, WRI's land and carbon lab and the CGIAR/CIAT MITIGATE+ project. Additionally, we extend special recognition to the dedicated teams involved in the design, collection, and administration of the field-based information used in this study from the National Forest and Wildlife Inventory (NF&WI) within the Peruvian Forest and Wildlife Service (SERFOR); the National Forest Resources Monitoring and Assessment (NAFORMA) program led by Tanzania Forest Services Agency, in collaboration with the FAO-Finland forestry program; Guyana's National Forest Carbon Monitoring System (FCMS) and the Guyana Forestry Commission; and the National Forest Inventory of Mozambique, particularly the Unidade de Monitoria, Relatório e Verificação (MRV) within the National Fund for Sustainable Development (FNDS).

Appendix. Supplementary data

Supplementary data to this article can be found online at $\frac{\text{https:}}{\text{doi.}}$ org/10.1016/j.scitotenv.2024.174653.

References

Aalde, H., Gonzalez, P., Gytarsky, M., Krug, T., Kurz, W.A., Ogle, S., Raison, J., Schoene, D., Ravindranath, N.H., Elhassan, N.G., Heath, L.S., Higuchi, N., Kainja, S., Matsumoto, M., Sanz Sánchez, M.J., Somogyi, Z. (Eds.), 2006. 2006 IPCC Guidelines for National Greenhouse Gas Inventories, vol. 4. National greenhouse gas inventories programme. IGES.

Alegria, J., 2020. Independent Evaluation of Mozambique National Activity Data Collection Protocols, Forest Inventory Design, and, Data Analysis. The World Bank -Mozambique. https://www.dropbox.com/s/nljyabynoo12fjj/Final_Report_Alegria. pdf?dl=0.

Araza, A., Herold, M., de Bruin, S., Ciais, P., Gibbs, D.A., Harris, N., Santoro, M., Wigneron, J.-P., Yang, H., Málaga, N., Nesha, K., Rodriguez-Veiga, P., Brovkina, O., Brown, H.C.A., Chanev, M., Dimitrov, Z., Filchev, L., Fridman, J., García, M., Hein, L., 2023. Past decade above-ground biomass change comparisons from four multi-temporal global maps. Int. J. Appl. Earth Obs. Geoinf. 118, 103274 https://doi.org/10.1016/j.jag.2023.103274.

- Avitabile, V., Herold, M., Heuvelink, G.B.M., Lewis, S.L., Phillips, O.L., Asner, G.P., Armston, J., Ashton, P.S., Banin, L., Bayol, N., Berry, N.J., Boeckx, P., de Jong, B.H. J., DeVries, B., Girardin, C.A.J., Kearsley, E., Lindsell, J.A., Lopez-Gonzalez, G., Lucas, R., Willcock, S., 2016. An integrated pan-tropical biomass map using multiple reference datasets. Glob. Chang. Biol. 22 (4), 1406–1420. https://doi.org/10.1111/ gcb.13139.
- Baccini, A., Goetz, S.J., Walker, W.S., Laporte, N.T., Sun, M., Sulla-Menashe, D., Hackler, J., Beck, P.S.A., Dubayah, R., Friedl, M.A., Samanta, S., Houghton, R.A., 2012. Estimated carbon dioxide emissions from tropical deforestation improved by carbon-density maps. Nat. Clim. Chang. 2 (3), 182–185. https://doi.org/10.1038/ nclimate1354.
- Brown, S., Goslee, K., Casarim, F., Harris, N., Petrova, S., 2014. Sampling design and implementation plan for Guyana's REDD+ Forest Carbon Monitoring System (FCMS): version 2. Winrock International.
- Bullock, E.L., Healey, S.P., Yang, Z., Acosta, R., Villalba, H., Insfrán, K.P., Melo, J., Wilson, S., Duncanson, L.I., Næsset, E., Armston, J., Saarela, S., Ståhl, G., Patterson, P.L., Dubayah, R., 2023. Estimating aboveground biomass density using hybrid statistical inference with GEDI lidar data and Paraguay's national forest inventory. Environ. Res. Lett. https://doi.org/10.1088/1748-9326/acdf03.
- Duncanson, L., Armston, J., Disney, M., Avitabile, V., Barbier, N., Calders, K., Carter, S., Chave, J., Herold, M., MacBean, N., McRoberts, R., Minor, D., Paul, K., Réjou-Méchain, M., Roxburgh, S., Williams, M., Albinet, C., Baker, T., Bartholomeus, H., Margolis, H., 2021. Aboveground woody biomass product validation: good practices protocol. In: Duncanson, L., Disney, M., Armston, J., Nickeson, J., Minor, D., Camacho, F. (Eds.), Land Product Validation Subgroup (WGCV/CEOS). https://doi.org/10.5067/doc/ceoswgcv/lpv/agb.001.
- Eggleston, H.S., Buendia, L., Miwa, K., Ngara, T., Tanabe, K. (Eds.), 2006. 2006 IPCC Guidelines for National Greenhouse Gas Inventories, vol. 1. National greenhouse gas inventories programme, IGES.
- FCPF, 2020. Carbon Fund Methodological Framework (Version 3). https://www.forestc arbonpartnership.org/system/files/documents/fcpf_carbon_fund_methodological_fr amework_revised_2020_final_posted.pdf.
- Feldpausch, T.R., Lloyd, J., Lewis, S.L., Brienen, R.J.W., Gloor, M., Monteagudo Mendoza, A., Lopez-Gonzalez, G., Banin, L., Abu Salim, K., Affum-Baffoe, K., Alexiades, M., Almeida, S., Amaral, I., Andrade, A., Aragão, L.E.O.C., Araujo Murakami, A., Arets, E.J.M.M., Arroyo, L., Aymard, C., G., A., Phillips, O.L., 2012. Tree height integrated into pantropical forest biomass estimates. Biogeosciences 9 (8), 3381–3403. https://doi.org/10.5194/bg.9-3381-2012.
- Fundo Nacional de Desenvolvimento Sustentavel. (n.d.). Story Map Series. Plataforma de acompanhamento dos Projectos do FNDS. Retrieved May 16, 2023, from https://www.arcgis.com/apps/MapSeries/index.html?appid=6602939f39ad4626a10 f87bf6253af1e.
- Government of Mozambique, 2018. Mozambique's Forest Reference Emission Level for Reducing Emissions from Deforestation in Natural Forests (Version 03). Ministry of Land, Environment and Rural Development, Republic of Mozambique. https://redd.unfcc.int/files/moz/frel/report final_v03_03102018.pdf.
- Government of the Cooperative Republic of Guyana, 2015. The Reference Level for Guyana's REDD+ Program. https://redd.unfccc.int/files/guyanas_proposal_for_reference_level_for_redd__final_sept_2015.pdf.
- Hunka, N., Santoro, M., Armston, J., Dubayah, R., McRoberts, R., Næsset, E., Quegan, S., Urbazaev, M., Pascual, A., May, P.B., Minor, D., Leitold, V., Basak, P., Liang, M., Melo, J., Herold, M., Malága, N., Wilson, S., Montesinos, P.D., Duncanson, L., 2023. On the NASA GEDI and ESA CCI biomass maps: aligning for uptake in the UNFCCC global stocktake. Environ. Res. Lett. https://doi.org/10.1088/1748-9326/ad0b60.
- Kyriakidis, P.C., 2004. A geostatistical framework for area-to-point spatial interpolation. Geogr. Anal. 36 (3), 259–289. https://doi.org/10.1111/j.1538-4632.2004.tb01135.
- Lawrence, M., McRoberts, R.E., Tomppo, E., Gschwantner, T., Gabler, K., 2010.
 Comparisons of National Forest Inventories. In: Tomppo, E., Gschwantner, T.,
 Lawrence, M., McRoberts, R.E. (Eds.), National Forest Inventories. Springer,
 Netherlands, pp. 19–32. https://doi.org/10.1007/978-90-481-3233-1_2.
 Lohr, S.L., 2010. Sampling: Design and Analysis, 2nd ed. Brooks/Cole.
- Málaga, N., de Bruin, S., McRoberts, R.E., Arana Olivos, A., de la Cruz Paiva, R., Durán Montesinos, P., Requena Suarez, D., Herold, M., 2022. Precision of subnational forest AGB estimates within the Peruvian Amazonia using a global biomass map. Int. J. Appl. Earth Observ. Geoinform. 115, 103102 https://doi.org/10.1016/j. iae.2022.103102.
- McRoberts, R.E., Tomppo, E.O., Schadauer, K., Ståhl, G., 2012. Harmonizing national forest inventories. For. Sci. 58 (3), 189–190. https://doi.org/10.5849/forsci.12-042.
- McRoberts, R.E., Liknes, G.C., Domke, G.M., 2014. Using a remote sensing-based, percent tree cover map to enhance forest inventory estimation. For. Ecol. Manage. 331, 12–18. https://doi.org/10.1016/j.foreco.2014.07.025.
- McRoberts, R.E., Chen, Q., Domke, G.M., Ståhl, G., Saarela, S., Westfall, J.A., 2016. Hybrid estimators for mean aboveground carbon per unit area. For. Ecol. Manage. 378, 44–56. https://doi.org/10.1016/j.foreco.2016.07.007.
- McRoberts, R.E., Næsset, E., Sannier, C., Stehman, S.V., Tomppo, E.O., 2020. Remote sensing support for the gain-loss approach for greenhouse gas inventories. Remote Sens. (Basel) 12 (11), 1891. https://doi.org/10.3390/rs12111891.
- McRoberts, R.E., Næsset, E., Heikkinen, J., Chen, Q., Strimbu, V., Esteban, J., Hou, Z., Giannetti, F., Mohammadi, J., Chirici, G., 2022. On the model-assisted regression estimators using remotely sensed auxiliary data. Remote Sens. Environ. 281, 113168 https://doi.org/10.1016/j.rse.2022.113168.
- McRoberts, R.E., Næsset, E., Heikkinen, J., Strimbu, V., 2024. Two-stage, model-assisted estimation using remotely sensed auxiliary data. Remote Sens. Environ. 307, 114125 https://doi.org/10.1016/j.rse.2024.114125.

- Melo, J., Baker, T., Nemitz, D., Quegan, S., Ziv, G., 2023. Satellite-based global maps are rarely used in forest reference levels submitted to the UNFCCC. Environ. Res. Lett. 18 (3), 034021 https://doi.org/10.1088/1748-9326/acba31.
- MINAGRI, & MINAM, 2016. Marco Metodológico del Inventario Nacional Forestal y de Fauna Silvestre Perú (Nº 253-2016-SERFOR-DE). Ministerio de Agricultura y Riego MINAGRI & Ministerio del Ambiente (MINAM), p. 38. http://www.serfor.gob.pe/portal/wp-content/uploads/2017/02/MARCO%20METODOLOGICO%20DEL%20 INFFS.pdf.
- $\label{eq:mitader} \begin{tabular}{ll} MITADER, 2018. Inventario Florestal Nacional, MITADER. https://www.fnds.gov.mz/mrv/index.php/documentos/relatorios/26-inventario-florestal-nacional/fileMaput florestal-nacional/fileMaput florestal-nacional/f$
- MNRT, 2015. National Forestry Resource Monitoring and Assessment of Tanzania (NAFORMA). Main Results. Ministry of Natural Resources & Tourism, Tanzania Forest Services (TFS) Agency, p. 106. http://www.fao.org/forestry/43612-09cf2f02 c20b55c1c00569e679197dcde.ndf.
- Næsset, E., Bollandsås, O.M., Gobakken, T., Solberg, S., McRoberts, R.E., 2015. The effects of field plot size on model-assisted estimation of aboveground biomass change using multitemporal interferometric SAR and airborne laser scanning data. Remote Sens. Environ. 168, 252–264. https://doi.org/10.1016/j.rse.2015.07.002.
- Næsset, E., Ørka, H.O., Solberg, S., Bollandsås, O.M., Hansen, E.H., Mauya, E., Zahabu, E., Malimbwi, R., Chamuya, N., Olsson, H., Gobakken, T., 2016. Mapping and estimating forest area and aboveground biomass in miombo woodlands in Tanzania using data from airborne laser scanning, TanDEM-X, RapidEye, and global forest maps: a comparison of estimated precision. Remote Sens. Environ. 175, 282–300. https://doi.org/10.1016/j.rse.2016.01.006.
- Næsset, E., McRoberts, R.E., Pekkarinen, A., Saatchi, S., Santoro, M., Trier, Ø.D., Zahabu, E., Gobakken, T., 2020. Use of local and global maps of forest canopy height and aboveground biomass to enhance local estimates of biomass in miombo woodlands in Tanzania. Int. J. Appl. Earth Observ. Geoinform. 93, 102138 https:// doi.org/10.1016/j.jag.2020.102138.
- Nesha, K., Herold, M., De Sy, V., De Bruin, S., Araza, A., Málaga, N., Gamarra, J.G.P., Hergoualc'h, K., Pekkarinen, A., Ramirez, C., Morales-Hidalgo, D., Tavani, R., 2022. Exploring characteristics of national forest inventories for integration with global space-based forest biomass data. Sci. Total Environ. 850, 157788 https://doi.org/ 10.1016/j.scitotenv.2022.157788.
- Ochiai, O., Poulter, B., Seifert, F.M., Ward, S., Jarvis, I., Whitcraft, A., Sahajpal, R., Gilliams, S., Herold, M., Carter, S., Duncanson, L.I., Kay, H., Lucas, R., Wilson, S.N., Melo, J., Post, J., Briggs, S., Quegan, S., Dowell, M., Rosenqvist, A., 2023. Towards a roadmap for space-based observations of the land sector for the UNFCCC global stocktake. iScience 26 (4), 106489. https://doi.org/10.1016/j.isci.2023.106489.
- Ogle, S., Kurz, W., Green, C., Brandon, A., Baldock, J., Domke, G., Herold, M., Bernoux, M., Chirinda, N., Ligt, R., Federici, S., García-Apaza, E., Grassi, G., Gschwantner, T., Hirata, Y., Houghton, R., House, J., Ishizuka, S., Jonckheere, I., Waterworth, R., 2019. Chapter 2 generic methodologies applicable to multiple landuse categories. In: 2019 Refinement to the 2006 IPCC Guidelines for National Greenhouse Gas Inventories, vol. 4. IPCC, pp. 2.1–2.96.
- Petrova, S., Goslee, K., Harris, N., Brown, S., 2013. Spatial Analysis for Forest Carbon Stratification and Sample Design for Guyana's FCMS: Version 2 [Technical report]. https://forestry.gov.gy/wp-content/uploads/2015/09/Guyana-Spatial-Analysis-for-Stratification-and-Sample-Plan-for-FCMS.pdf.
- Plataforma Geobosques, 2021. Mapas de Uso y Cambio de Uso Periodo 2013–2016 [Map]. Programa Nacional de Conservación de Bosques para la Mitigación del Cambio Climático, Ministerio del Ambiente. http://geobosques.minam.gob.pe/geobosque/view/descargas.php?122345gxxe345w34gg.
- Réjou-Méchain, M., Muller-Landau, H.C., Detto, M., Thomas, S.C., Le Toan, T., Saatchi, S. S., Barreto-Silva, J.S., Bourg, N.A., Bunyavejchewin, S., Butt, N., Brockelman, W.Y., Cao, M., Cárdenas, D., Chiang, J.-M., Chuyong, G.B., Clay, K., Condit, R., Dattaraja, H.S., Davies, S.J., Chave, J., 2014. Local spatial structure of forest biomass and its consequences for remote sensing of carbon stocks. Biogeosciences 11 (23), 6827–6840. https://doi.org/10.5194/bg-11-6827-2014.
- Réjou-Méchain, M., Tanguy, A., Piponiot, C., Chave, J., Hérault, B., 2017. BIOMASS: an R package for estimating above-ground biomass and its uncertainty in tropical forests. Methods Ecol. Evol. 8 (9), 1163–1167. https://doi.org/10.1111/2041-210X.12753.
- Réjou-Méchain, M., Barbier, N., Couteron, P., Ploton, P., Vincent, G., Herold, M., Mermoz, S., Saatchi, S., Chave, J., de Boissieu, F., Féret, J.-B., Takoudjou, S.M., Pélissier, R., 2019. Upscaling forest biomass from field to satellite measurements: sources of errors and ways to reduce them. Surv. Geophys. 40 (4), 881–911. https:// doi.org/10.1007/s10712-019-09532-0.
- Romijn, E., Lantican, C.B., Herold, M., Lindquist, E., Ochieng, R., Wijaya, A., Murdiyarso, D., Verchot, L., 2015. Assessing change in national forest monitoring capacities of 99 tropical countries. For. Ecol. Manage. 352, 109–123. https://doi. org/10.1016/j.foreco.2015.06.003.
- Saarela, S., Schnell, S., Tuominen, S., Balázs, A., Hyyppä, J., Grafström, A., Ståhl, G., 2016. Effects of positional errors in model-assisted and model-based estimation of growing stock volume. Remote Sens. Environ. 172, 101–108. https://doi.org/ 10.1016/j.rse.2015.11.002.
- Saatchi, S., Harris, N.L., Brown, S., Lefsky, M., Mitchard, E.T.A., Salas, W., Zutta, B.R., Buermann, W., Lewis, S.L., Hagen, S., Petrova, S., White, L., Silman, M., Morel, A., 2011. Benchmark map of forest carbon stocks in tropical regions across three continents. Proc. Natl. Acad. Sci. 108 (24), 9899–9904. https://doi.org/10.1073/pnas.1019576108.
- Santoro, M., Cartus, O., 2023. ESA Biomass Climate Change Initiative (Biomass_cci): Global Datasets of Forest Above-ground Biomass for the Years 2010, 2017, 2018, 2019 and 2020, v4. NERC EDS Centre for Environmental Data Analysis. https://doi.org/10.5285/AF60720C1E404A9E9D2C145D2B2EAD4E (p. 5183 Files, 302039459020 B) [Application/xml].

- Santoro, M., Cartus, O., Mermoz, S., Bouvet, A., Le Toan, T., Carvalhais, N., Rozendaal, D., Herold, M., Avitabile, V., Quegan, S., Carreiras, J., Rauste, Y., Balzter, H., Schmullius, C., Seifert, F.M., 2018. GlobBiomass—Global Datasets of Forest Biomass (p. 174 data points) [Text/tab-separated-values]. PANGAEA - Data Publisher for Earth & Environmental Science. https://doi.org/10.1594/ PANGAEA.894711.
- Särndal, C.-E., Swensson, B., Wretman, J., 1992. Model Assisted Survey Sampling. Springer.
- SERFOR, 2016. Cluster [Capa de polígonos de Geodatabase]. En Geodatabase de la Dirección de Inventario y Valoración del SERFOR (En Geodatabase de la Dirección de Inventario y Valoración del SERFOR).
- SERFOR, 2020. Inventario nacional forestal y de fauna silvestre: Informe de resultados del panel 1. https://www.serfor.gob.pe/portal/wp-content/uploads/2020/09/Infor me-del-Inventario-Nacional-Forestal-y-de-Fauna-Silvestre-Panel-1-Versi%C3%B3n-a migable.pdf.
- Ståhl, G., Saarela, S., Schnell, S., Holm, S., Breidenbach, J., Healey, S.P., Patterson, P.L., Magnussen, S., Næsset, E., McRoberts, R.E., Gregoire, T.G., 2016. Use of models in large-area forest surveys: comparing model-assisted, model-based and hybrid estimation. Forest Ecosyst. 3 (1), 5. https://doi.org/10.1186/s40663-016-0064-9.

- Tomppo, E., Gschwantner, T., Lawrence, M., McRoberts, R.E. (Eds.), 2010. National Forest Inventories: Pathways for Common Reporting. Springer Netherlands. https://doi.org/10.1007/978-90-481-3233-1.
- Tomppo, E., Malimbwi, R., Katila, M., Mäkisara, K., Henttonen, H.M., Chamuya, N., Zahabu, E., Otieno, J., 2014. A sampling design for a large area forest inventory: case Tanzania. Can. J. For. Res. 44 (8), 931–948. https://doi.org/10.1139/cjfr-2013-0490.
- Tomppo, E., Kuusinen, N., Mäkisara, K., Katila, M., McRoberts, R.E., 2017. Effects of field plot configurations on the uncertainties of ALS-assisted forest resource estimates. Scand. J. For. Res. 32 (6), 488–500. https://doi.org/10.1080/ 02827581.2016.1259425.
- URT, 2010. National Forestry Resource Monitoring and Assessment of Tanzania (NAFORMA). Field Manual. Biophysical Survey. Ministry of Natural Resources & Tourism, The United Republic of Tanzania, p. 95. http://www.fao.org/forestry/23484-05b4a32815ecc769685b21b03be44ea77.pdf.
- Zeileis, A., Hothorn, T., 2002. Diagnostic checking in regression relationships. R News 2 (3), 7–10. https://CRAN.R-project.org/doc/Rnews/.